Topological phase transitions and universality in the Haldane-Hubbard model

Alessandro Giuliani,[1] Ian Jauslin,[2] Vieri Mastropietro,[3] and Marcello Porta[3]

[1] *University of Roma Tre, L.go S. L. Murialdo 1, 00146 Rome, Italy*
[2] *University of Zürich, Winterthurerstrasse 190, 8057 Zürich, Switzerland*
[3] *University of Milan, Via Saldini 50, Milan, Italy*

We study the Haldane-Hubbard model by exact Renormalization Group techniques. We construct the topological phase diagram, for weak interactions. We predict that many-body interactions induce a shift of the transition line. The presence of new intermediate phases, absent in the non interacting case, is rigorously excluded at weak coupling. Despite the nontrivial renormalization of the wave function and of the Fermi velocity, the conductivity is universal: at the renormalized critical line, both the discontinuity of the transverse conductivity and the longitudinal conductivity do not depend on the interaction, thanks to remarkable cancellations due to lattice Ward Identities.

PACS numbers: 73.43.Nq, 05.30.Fk, 71.10.Fd, 73.43.-f, 05.10.Cc, 05.30.Rt

I. INTRODUCTION

The current understanding of topological matter[1,2] is mostly based on a single-particle description. A paradigmatic example is the integer quantum Hall effect: in the absence of interactions, the Hall conductivity has a deep topological interpretation[3,4], which explains its quantization and stability. A more recent example is provided by the classification of time-reversal invariant insulators[5,6] and by the identification of the corresponding geometrical indices[7–9], which, again, rely on the properties of the noninteracting Bloch functions. In general, the topological classification explains the stability of charge or spin transport against perturbations that preserve the insulating nature of the system, and respect its basic symmetries. These ideas, however, do not do not apply to systems with many-body interactions. Understanding the effect of interactions on this classification is a major open problem.

Simple, yet profound models, like the Haldane model[10], have played an important role in recent developments. In the absence of interactions, this model has a nontrivial topological phase diagram, which can be analytically computed. Due to its simplicity, it provides a good platform to test and calibrate numerical techniques and approximate analytical schemes, that are used for more realistic systems. The Haldane model has been experimentally realized using cold atoms in optical lattices[11]: the critical lines separating distinct topological phases have been measured and shown to be in agreement with the theoretical predictions. Such experiments can include an on-site tunable interaction between electrons, therefore, it is likely that future measurements will shed light on the effect of interactions on the topological phase diagram.

A major question is whether interactions can produce new topological phases with respect to the single-particle picture. In the Haldane-Hubbard model, such phases have been predicted by mean-field theory arguments[12–17], the variational cluster method[18,19], the slave-rotor and slave-spin approaches[20,21], numerical diagonalization[22–26] and dynamical mean field theory[25,26] . However, all such methods have limitations, due to the small number of degrees of freedom and to uncontrolled approximations. For instance, exact diagonalization results predict the presence of a new phase even at weak interaction, although this is believed to be a spurious phenomenon due to finite size effects[23,26]. Therefore, it is of crucial importance to develop *exact* theoretical methods, that may check the validity of numerical predictions, at least for some range of parameters. Note that, in the case of *gapped* systems, well-known theoretical arguments[27–29] ensure the stability of topological phases, but these methods break down near transition lines, at which gaps are, typically, closed.

In this paper we derive a number of exact analytical predictions for the Haldane-Hubbard model, by using constructive Renormalization Group[30–33] methods. These allow us to determine the phase diagram and correlation functions at weak coupling. We rigorously prove that the interaction does not produce any new phase; non-perturbative effects are rigorously excluded by the convergence of the renormalized series. However, the interaction produces a deformation of the topological phase boundary, see Fig.1 below. In particular, the topologically non-trivial phase is *amplified* by the presence of weak repulsive interactions, which is consistent with recent numerical analyses[16,26]. An analogous stabilization phenomenon of the topological phase due to interactions has been discussed in more general topological models, both in two and three dimensions[34]. In the vicinity of the phase boundaries, the approximate description of the model in terms of massive Dirac fermions is affected by a non-trivial renormalization of the coefficients: besides a renormalization of the Fermi velocity, there are *two* different wave function renormalizations, one for each pseudo-spin index (see Fig.2). However, despite the non-universal form of the renormalized propagator and the shift of the transition line, the conductivity at criticality is *universal*: all interaction corrections cancel out exactly, thanks to lattice Ward identities, following from exact conservation laws. More precisely, both the discontinuity of the transverse conductivity and the longitudinal

conductivity at the critical line are independent of the interaction.

In order to describe our results in more detail, we recall that the Haldane-Hubbard model is

$$H = H_0 + U \sum_{\vec{x}\in\Lambda_A\cup\Lambda_B} \Big(n_{\vec{x},\uparrow} - \frac{1}{2}\Big)\Big(n_{\vec{x},\downarrow} - \frac{1}{2}\Big) - \mu N \ , \quad (1)$$

where $H_0 = H_0(t_1, t_2, W, \phi)$ is the hopping Hamiltonian on the honeycomb lattice (see eq.(4) below), where $t_{1,2}$ are the strengths of the nearest neighbor and next-to-nearest neighbor hoppings, $\pm\phi$ is the complex phase of the next-to-nearest neighbor hopping, and W the half-amplitude of the staggered potential. Moreover, $\Lambda_{A/B}$ are the A/B sub-lattices of the honeycomb lattice, $n_{\vec{x},\sigma}$ the number operators for electrons with spin σ at site $\vec{x}$, and μ is the chemical potential, fixed in such a way that the Fermi energy is in between the valence and conduction bands.

If $U = 0$, the non-interacting critical line is $W \pm 3\sqrt{3}\, t_2 \sin\phi = 0$, whose complement consists of four disconnected regions, two of which are trivial (zero Chern number), while the other two are characterized by a non-vanishing Hall conductivity. On the component of the critical line $m_\omega \equiv W + \omega 3\sqrt{3}\, t_2 \sin\phi = 0$, with $\omega \in \{\pm\}$, the propagator is singular at the Fermi point $\vec{p}_F^{\,\omega} = (\frac{2\pi}{3}, \omega\frac{2\pi}{3\sqrt{3}})$. In the vicinity of this component, the non-interacting propagator is

$$\hat{S}_2(k_0, \vec{p}_F^{\,\omega} + \vec{k}')\big|_{U=0} \simeq \\ \simeq \begin{pmatrix} -ik_0 + m_\omega & -\frac{3}{2}t_1(-ik'_1 + \omega k'_2) \\ -\frac{3}{2}t_1(ik'_1 + \omega k'_2) & -ik_0 - m_\omega \end{pmatrix}^{-1} ,$$

up to higher order terms in the Matsubara frequency k_0 and in the quasi-momentum $\vec{k}'$. Our main results are the following:

1. The topological phase boundary is *not* universal but, rather, it is modified non-trivially by the interaction. The interacting critical line is the solution of the implicit equation

$$m_{\pm,R} = W \pm 3\sqrt{3}\, t_2 \sin\phi - F_\pm(U, W, \phi) = 0 \quad (2)$$

where $F_\pm(U, W, \phi)$ are analytic functions of U, derived below in the form of *convergent* renormalized series, see Section III below. The solution of the fixed point equation above is plotted in Fig.1. Remarkably, our calculation predicts that at weak coupling the repulsive interaction favors topological order, i.e., the non-trivial Chern phase is amplified by the presence of a small, positive U.

2. The interaction modifies the 2-point function producing non trivial U-dependent renormalization of the parameters

$$\hat{S}_2(k_0, \vec{p}_F^{\,\omega} + \vec{k}') \simeq \\ \simeq \begin{pmatrix} -ik_0 Z_{1,R} + m_{\omega,R} & -v_R(-ik'_1 + \omega k'_2) \\ -v_R(ik'_1 + \omega k'_2) & -ik_0 Z_{2,R} - m_{\omega,R} \end{pmatrix}^{-1} ,$$

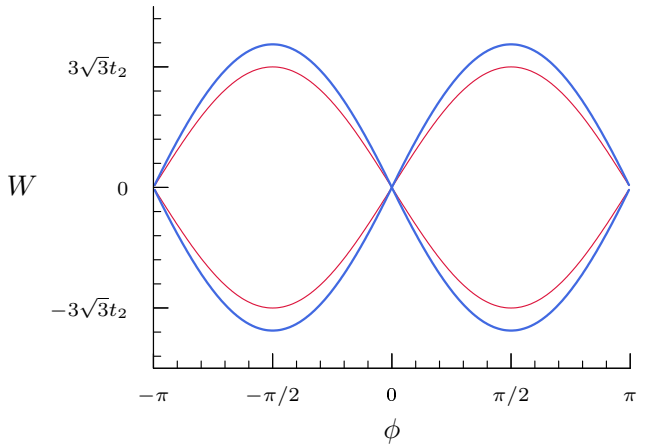

FIG. 1. Renormalization of the critical curve. The inner curve is the unperturbed one, while the outer one is the renormalized curve (at first order in perturbation theory), with $t_1 = 1, t_2 = 0.1, U = 0.5$

up to higher order corrections in $(k_0, \vec{k}')$. In this formula, $Z_{\rho,R}$ and v_R are, respectively, the wave function renormalizations and the dressed Fermi velocity. In contrast to the non-interacting model, as well as to the predictions of the effective interacting Dirac theory, the velocity is modified and $Z_{1,R} \neq Z_{2,R}$ in general (see Fig.2), with the exception of four special highly symmetric points ($\phi = 0, \pi, \pm\pi/2$, see below).

3. The Hall conductivity is *exactly* quantized, even in the presence of interactions, arbitrarily close to the renormalized critical lines. In other words, while the transition lines are non-universal, and the dressed propagator has a symmetry structure that is different from the non-interacting one, the discontinuity of the Hall conductivity across the line is universal. Moreover, the value of the longitudinal conductivity on the critical line is non-vanishing and universal. The universal quantization of these conductivities comes from remarkable cancellations, implied by exact lattice Ward Identities. For instance, the transverse conductivity is

$$\sigma_{12} = 2 \lim_{p_0\to 0^+} \int \frac{d\mathbf{k}}{(2\pi)^3} \times \quad (3) \\ \times \mathrm{Tr}\big\{\hat{S}_2(\mathbf{k})\hat{\Gamma}_1(\mathbf{k})\partial_{p_0}\hat{S}_2(\mathbf{k} + (p_0, \vec{0}))\hat{\Gamma}_2(\mathbf{k})\big\},$$

where $\hat{S}_2(\mathbf{k})$ is the dressed propagator, and $\hat{\Gamma}_i(\mathbf{k})$ the dressed vertex function, which are both non-trivial functions of the coupling. Lattice Ward Identities guarantee non-perturbative cancellations among the contributions to the dressed propagator and vertex functions, which imply the universal quantization of the jump of σ_{12} across the critical line, equal to $\pm 1/\pi$, as in the non-interacting

model. Similarly, the longitudinal conductivity on the critical line is equal to 1/8 at all points except $W = \phi = 0$, where the value is 1/4.

The results above are obtained by an exact Renormalization Group analysis, valid at, and arbitrarily close to, the topological phase boundary, where the system becomes massless. Note that naive perturbation theory breaks down at the phase boundaries, even at weak coupling, because of the corrections of the critical line, due to the interaction. In order to get unambiguous results, we perform a renormalized expansion around the interacting critical line, which is determined in a self-consistent way. All the physical quantities are written in terms of the renormalized expansion, which is rigorously proved to be *convergent* in the weak coupling regime. The expansion we use is based on the mathematical methods of constructive field theory[30–33], which allow us to systematically take all the lattice effects into account, with rigorous bounds on the errors produced by finite truncations in the renormalized expansion. For earlier applications of the method to interacting graphene, see Ref.[35,36].

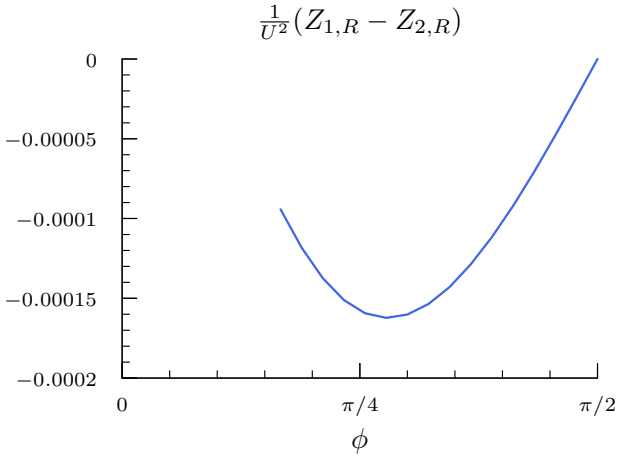

FIG. 2. The difference $(Z_{1,R} - Z_{2,R})/U^2$ between the two wave function renormalizations corresponding to the two sublattices of the honeycomb lattice, at second order in perturbation theory, along the critical curve, plotted as a function of ϕ, with $t_1 = 1, t_2 = 0.1$.

In the following, we describe the model, its symmetries, and the constructive technique leading us to the proof of these results, in more detail. The paper is organized as follows. In Section II we define the Haldane-Hubbard model, and derive the exact lattice Ward Identities for its correlation functions. In Section III we perform an exact Renormalization Group analysis for the correlations, and compute the decay of the correlations at large distances, as well as the renormalized critical line. In Section IV we prove the quantization of the Hall conductivity across the critical line.

II. THE HALDANE-HUBBARD MODEL

The Haldane-Hubbard model is defined by the Hamiltonian (1), with

$$H_0 = \sum_{\vec{x}\in\Lambda_A}\sum_{\sigma=\uparrow\downarrow}\sum_{j=1,2,3}\Big[- t_1\Big(a^+_{\vec{x},\sigma}b^-_{\vec{x}+\vec{\delta}_j,\sigma} + b^+_{\vec{x}+\vec{\delta}_j,\sigma}a^-_{\vec{x},\sigma}\Big)$$
$$-t_2\sum_{\alpha=\pm}\Big(e^{i\alpha\phi}a^+_{\vec{x},\sigma}a^-_{\vec{x}+\alpha\vec{\gamma}_j,\sigma} + e^{-i\alpha\phi}b^+_{\vec{x}+\vec{\delta}_1,\sigma}b^-_{\vec{x}+\vec{\delta}_1+\alpha\vec{\gamma}_j,\sigma}\Big)$$
$$+\frac{W}{3}\Big(a^+_{\vec{x},\sigma}a^-_{\vec{x},\sigma} - b^+_{\vec{x}+\vec{\delta}_j,\sigma}b^-_{\vec{x}+\vec{\delta}_j,\sigma}\Big)\Big] . \qquad (4)$$

Here, $\Lambda_A \cup \Lambda_B$ is the honeycomb lattice, whose lattice spacing is normalized to one, thought of as the union of two translated copies Λ_A and $\Lambda_B = \Lambda_A + (1, 0)$ of the triangular lattice generated by $\vec{\ell}_{1,2} = \frac{1}{2}(3, \mp\sqrt{3})$. The nearest neighbor vectors of the honeycomb lattice are denoted by $\vec{\delta}_j$, and the next-to-nearest neighbor vectors are $\vec{\gamma}_j$, see Fig.3. The operators $a^\pm_{\vec{x},\sigma}$ and $b^\pm_{\vec{x},\sigma}$ denote creation/annihilation operators of electrons sitting on the sites of the A and B sublattices. Moreover, $n_{\vec{x},\sigma} = a^+_{\vec{x},\sigma}a^-_{\vec{x},\sigma}$ (resp. $n_{\vec{x},\sigma} = b^+_{\vec{x},\sigma}b^-_{\vec{x},\sigma}$) if $\vec{x} \in \Lambda_A$ (resp. $\vec{x} \in \Lambda_B$), μ is the chemical potential and N the total number operator. We also introduce a finite volume approximation of H with periodic boundary conditions, denoted by H_L, which is defined in the same way as H, with Λ_A replaced by the torus $\Lambda^{(L)}_A = \Lambda_A/L\Lambda_A$, and similarly for Λ_B. Finally, we let $\langle\cdot\rangle_\beta$ be the Gibbs state of H at inverse temperature β, obtained as the infinite volume limit of the one associated with H_L, namely $\langle\cdot\rangle_\beta = \lim_{L\to\infty}\langle\cdot\rangle_{\beta,L}$, with $\langle\cdot\rangle_{\beta,L} = \mathrm{Tr}\{e^{-\beta H_L}\cdot\}/\mathrm{Tr}\{e^{-\beta H_L}\}$. The thermal ground state of H is defined as $\langle\cdot\rangle = \lim_{\beta\to\infty}\langle\cdot\rangle_\beta$.

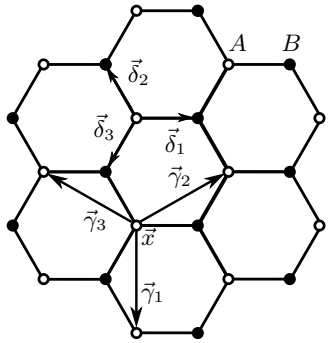

FIG. 3. The honeycomb lattice of the Haldane-Hubbard model with its A and B sublattices.

Correlations, current and conductivity. We define $\Psi^+_{\vec{x},\sigma} = \big(a^+_{\vec{x},\sigma}, b^+_{\vec{x}+\vec{\delta}_1,\sigma}\big)$, $\Psi^-_{\vec{x},\sigma} = \big(\Psi^+_{\vec{x},\sigma}\big)^\dagger$ and, for any inverse temperature β, we let $\Psi^\pm_{\vec{x},\sigma}(x_0) = e^{Hx_0}\Psi^\pm_{\vec{x},\sigma}e^{-Hx_0}$ be their evolution at 'imaginary time' $x_0 \in [0, \beta)$. For general $x_0 \in \mathbb{R}$, we extend $\Psi^\pm_{\vec{x},\sigma}(x_0)$ anti-periodically (of anti-period β) beyond the basic interval $[0, \beta)$. The Fourier transform of the fields is defined via $\Psi^\pm_{\vec{x},\sigma} = \int_{\mathcal{B}}\frac{d\vec{k}}{|\mathcal{B}|}e^{\pm i\vec{k}\cdot\vec{x}}\hat{\Psi}^\pm_{\vec{k},\sigma}$, where $\mathcal{B}$ is the Brillouin zone[37]. The

2-point function is

$$S_2(\mathbf{x},\mathbf{y}) = \langle \mathbf{T}\, \Psi^-_{\vec{x},\sigma}(x_0)\Psi^+_{\vec{y},\sigma}(y_0)\rangle = \int_{\mathbb{R}\times\mathcal{B}} \frac{d\mathbf{k}}{2\pi|\mathcal{B}|} e^{-i\mathbf{k}(\mathbf{x}-\mathbf{y})}\hat{S}_2(\mathbf{k}),$$

where $\mathbf{x}=(x_0,\vec{x})$, $\mathbf{y}=(y_0,\vec{y})$, $\mathbf{T}$ is the fermionic time-ordering operator (which orders imaginary times in decreasing order[38]), and $\mathbf{k}=(k_0,\vec{k})$, where k_0 is the Fourier dual of the imaginary time (the 'Matsubara frequency'). Note that S_2 is a 2×2 matrix (with indices in the 'sublattice' space) and its definition is independent of the choice of $\sigma\in\{\uparrow,\downarrow\}$.

The current is defined via the Peierls' substitution (see App.A), and is equal to

$$\vec{J}_{\vec{p}}(x_0) = \sum_{\sigma=\uparrow\downarrow}\int_{\mathcal{B}} \frac{d\vec{k}}{|\mathcal{B}|}\hat{\Psi}^+_{\vec{k}+\vec{p},\sigma}(x_0)\vec{M}(\vec{k},\vec{p})\hat{\Psi}^-_{\vec{k},\sigma}(x_0)\ . \quad (5)$$

The two components $M_i(\vec{k},\vec{p})$, $i=1,2$, of $\vec{M}(\vec{k},\vec{p})$ are the bare vertex functions, which are 2×2 matrices, with elements labelled by the spinor indices. For the explicit expression of the bare vertex functions, see App.A.

The current-current and the vertex correlations are defined, respectively, as

$$\hat{K}_{\mu\nu}(\mathbf{p}) = \int_{\mathbb{R}} dx_0 e^{-ip_0x_0}\langle\!\langle \mathbf{T}\, J_{\vec{p},\mu}(x_0); J_{-\vec{p},\nu}(0)\rangle\!\rangle_\infty,$$
$$\hat{G}_\mu(\mathbf{k},\mathbf{p}) = \int_{\mathbb{R}} dx_0 \int_{\mathbb{R}} dy_0\, e^{-ip_0x_0+i(k_0+p_0)y_0}\times \times\langle\!\langle \mathbf{T}\, J_{\vec{p},\mu}(x_0); \hat{\Psi}^-_{\vec{k}+\vec{p},\sigma}(y_0)\hat{\Psi}^+_{\vec{k},\sigma}\rangle\!\rangle_\infty, \quad (6)$$

where $\mu,\nu\in\{0,1,2\}$,

$$J_{\vec{p},0}(x_0) = \sum_{\vec{x}\in\Lambda_A}\sum_{\sigma=\uparrow\downarrow} e^{-i\vec{p}\cdot\vec{x}}\Psi^+_{\vec{x},\sigma}(x_0)M_0(\vec{p})\Psi^-_{\vec{x},\sigma}(x_0),$$

with $\big[M_0(\vec{p})\big]_{\rho,\rho'} = \delta_{\rho,\rho'}e^{-i\vec{p}\vec{\delta}_1(\rho-1)}$, and $J_{\vec{p},i}(x_0)$, with $i=1,2$, are the two components of the current in eq.(5). Moreover, $\langle\!\langle\cdot\rangle\!\rangle_\infty = \lim_{\beta\to\infty}\lim_{L\to\infty} L^{-2}\langle\cdot\rangle_{\beta,L}$ is the trace per unit volume, and the semi-colon indicates that the expectation is truncated: $\langle\!\langle \mathbf{T}\, A(x_0);B(y_0)\rangle\!\rangle_\infty = \langle\!\langle \mathbf{T}\, A(x_0)B(y_0)\rangle\!\rangle_\infty - \langle\!\langle A\rangle\!\rangle_\infty\langle\!\langle B\rangle\!\rangle_\infty$, where $A(x_0)$ and $B(y_0)$ are the imaginary time evolutions of two extensive observables A and B.

For later reference, we also introduce the vertex function:

$$\hat{\Gamma}_\mu(\mathbf{k},\mathbf{p}) = \hat{S}_2^{-1}(\mathbf{k}+\mathbf{p})\hat{G}_\mu(\mathbf{k},\mathbf{p})\hat{S}_2^{-1}(\mathbf{k}), \quad (7)$$

where $\hat{S}_2^{-1}(\mathbf{k})$ is the inverse of the 2-point function, thought of as a 2×2 matrix.

Finally, the d.c. Kubo conductivity is defined in terms of the current-current correlation as

$$\sigma_{ij} = -\lim_{p_0\to 0^+}\frac{1}{Ap_0}\big[\hat{K}_{ij}(p_0,0)-\hat{K}_{ij}(\mathbf{0})\big], \quad (8)$$

where $i,j=1,2$ and $A=|\vec{\ell}_1\times\vec{\ell}_2| = 3\sqrt{3}/2$ is the area of the fundamental cell.

Ward Identities. The continuity equation for the lattice current eq.(5), when averaged against an arbitrary number of field operators, implies exact identities among correlation functions (Ward Identities), valid for any value of the interaction U. In particular, the one relating the 2-point and the vertex functions, which will play an important role in the following, reads as follows:

$$\sum_{\mu=0}^{2}(i)^{\delta_{\mu,0}}p_\mu\hat{G}_\mu(\mathbf{k},\mathbf{p}) = \hat{S}_2(\mathbf{k}+\mathbf{p})M_0(\vec{p}) - M_0(\vec{p})\hat{S}_2(\mathbf{k}). \quad (9)$$

If we derive this equation with respect to $\mathbf{p}$, compute the result at $\mathbf{p}=\mathbf{0}$ and recall the definition (7) of the vertex function, we find:

$$\hat{\Gamma}_\mu(\mathbf{k},\mathbf{0}) = (-i)^{\delta_{\mu,0}}\partial_\mu\hat{S}_2^{-1}(\mathbf{k}) + \big[\partial_\mu M_0(\vec{0}),\hat{S}_2^{-1}(\mathbf{k})\big]. \quad (10)$$

In the following, $\hat{\Gamma}_\mu(\mathbf{k},\mathbf{0})$ will be denoted simply by $\hat{\Gamma}_\mu(\mathbf{k})$, which is the same function as that appearing in eq.(3).

The non-interacting case. If $U=0$, the band structure and the phase diagram can be computed explicitly: the Bloch Hamiltonian is

$$\hat{H}_0(\vec{k}) = \quad (11)$$
$$= \begin{pmatrix} -2t_2\cos\phi\,\alpha_1(\vec{k}) + m(\vec{k}) & -t_1\Omega^*(\vec{k}) \\ -t_1\Omega(\vec{k}) & -2t_2\cos\phi\,\alpha_1(\vec{k}) - m(\vec{k})\end{pmatrix}$$

with $\alpha_1(\vec{k}) = \sum_{j=1}^3\cos(\vec{k}\cdot\vec{\gamma}_i)$, $\alpha_2(\vec{k}) = \sum_{j=1}^3\sin(\vec{k}\cdot\vec{\gamma}_i)$, $m(\vec{k}) = W - 2t_2\sin\phi\,\alpha_2(\vec{k})$ and $\Omega(\vec{k}) = 1 + e^{-i\vec{k}\cdot\vec{\ell}_1} + e^{-i\vec{k}\cdot\vec{\ell}_2}$. The corresponding energy bands are

$$\varepsilon_\pm(\vec{k}) = -2t_2\cos\phi\,\alpha_1(\vec{k}) \pm \sqrt{m(\vec{k})^2 + t_1^2|\Omega(\vec{k})|^2}\ .$$

To make sure that the energy bands do not overlap, we assume that $t_2/t_1 < 1/3$. The two bands can only touch at the *Fermi points* $\vec{p}_F^{\,\pm} = \big(\frac{2\pi}{3}, \pm\frac{2\pi}{3\sqrt{3}}\big)$, which are the two zeros of $\Omega(\vec{k})$, around which $\Omega(\vec{p}_F^{\,\pm}+\vec{k}') \simeq \frac{3}{2}(ik_1' \pm k_2')$. The condition that the two bands touch at $\vec{p}_F^{\,\omega}$, with $\omega\in\{+,-\}$, is that $m_\omega = 0$, with

$$m_\omega := m(\vec{p}_F^{\,\omega}) = W + \omega 3\sqrt{3}\,t_2\sin\phi\ .$$

The unperturbed critical line is, therefore, $\{(\phi,W) : W = \pm 3\sqrt{3}\,t_2\sin\phi\}$. Fixing the chemical potential in such a way that the Fermi energy lies in between the two bands, $\mu = -2t_2\cos\phi\,\alpha_1(\vec{p}_F^{\,\pm}) = -3t_2\cos\phi$, the system passes from a semi-metallic behavior, when (ϕ,W) is on the critical line, to an insulating behavior, characterized by the exponential decay of correlations, when $W\neq\pm 3\sqrt{3}t_2\,\sin\phi$.

The insulating phase consists of four disconnected regions in the (ϕ,W) plane, two of which are 'topologically trivial', while the other two have non-zero Hall conductivity: more precisely, if $W\neq\pm 3\sqrt{3}t_2\,\sin\phi$,

$$\sigma_{12} = \frac{1}{2\pi}\big[\mathrm{sign}(m_-) - \mathrm{sign}(m_+)\big]\ .$$

III. RENORMALIZATION GROUP ANALYSIS

We now construct the interacting correlations and phase diagram, by using a convergent renormalized expansion, in the spirit of Ref.[29,35,36]. In this section, we introduce the functional integral formulation of the model, discuss the exact lattice symmetries of the fermionic action, and describe the infrared integration, including the study of the flow of the running coupling constants. One of the main results of this section is the equation for the interacting critical line.

A. Functional integral formulation

We are interested in the semi-metallic and insulating regimes of the interacting system. We, therefore, set the chemical potential accordingly (its value will be different, in general, from the unperturbed one):

$$\mu = -2t_2 \cos\phi\alpha_1(\vec{p}_F^{\pm}) - \nu,$$

with ν to be chosen as a function of U, W, ϕ, so that the renormalized propagator either has a linear, 'conical', infrared singularity (along the interacting critical line), or is gapped (in the insulating phase).

The generating function $\mathcal{W}(f, A)$ for correlations, in which f is the external field conjugated to $\Psi^{\pm}_{\vec{x},\sigma}(x_0)$, and A is the external field conjugated to the current, can be written as the following Grassmann integral:

$$e^{\mathcal{W}(f,A)} = \frac{\int P(d\psi) e^{-V(\psi)+(\psi,f)+(j,A)}}{\int P(d\psi) e^{-V(\psi)}}, \qquad (12)$$

where: $\psi^{\pm}_{\mathbf{x},\sigma}$, with $\mathbf{x} = (x_0, \vec{x}) \in \mathbb{R} \times \Lambda_A$ and $\sigma \in \{\uparrow, \downarrow\}$, is a two-component Grassmann spinor (it is the Grassmann counterpart of $\Psi^{\pm}_{\vec{x},\sigma}(x_0)$), whose components will be denoted $\psi^{\pm}_{\mathbf{x},\sigma,\rho}$, with $\rho = 1, 2$; $P(d\psi)$ is the fermionic Gaussian integration with propagator

$$g(\mathbf{x}, \mathbf{y}) = \int_{\mathbb{R}\times\mathcal{B}} \frac{d\mathbf{k}}{2\pi|\mathcal{B}|} e^{-i\mathbf{k}(\mathbf{x}-\mathbf{y})} \hat{g}(\mathbf{k}), \qquad (13)$$

where, letting $R(\vec{k}) = -2t_2 \cos\phi\big(\alpha_1(\vec{k}) - \alpha_1(\vec{p}_F^{\pm})\big)$,

$$\hat{g}(\mathbf{k}) = \begin{pmatrix} -ik_0 + R(\vec{k}) + m(\vec{k}) & -t_1\Omega^*(\vec{k}) \\ -t_1\Omega(\vec{k}) & -ik_0 + R(\vec{k}) - m(\vec{k}) \end{pmatrix}^{-1}$$

and, at contact, $g(\mathbf{x}, \mathbf{x})$ should be interpreted as $\lim_{\varepsilon\to 0^+}[g(\mathbf{x} + (\varepsilon, \vec{0}), \mathbf{x}) + g(\mathbf{x} - (\varepsilon, \vec{0}), \mathbf{x})]$;

$$V(\psi) = \int_{\mathbb{R}} dx_0 \sum_{\vec{x}\in\Lambda_A} \sum_{\rho=1,2} \big(U n^{\rho}_{\mathbf{x},\uparrow} n^{\rho}_{\mathbf{x},\downarrow} + \nu \sum_{\sigma=\uparrow,\downarrow} n^{\rho}_{\mathbf{x},\sigma}\big),$$

where $n^{\rho}_{\mathbf{x},\sigma} = \psi^{+}_{\mathbf{x},\sigma,\rho}\psi^{-}_{\mathbf{x},\sigma,\rho}$; and, finally,

$$(\psi, f) = \int_{\mathbb{R}} dx_0 \sum_{\vec{x}\in\Lambda_A} \sum_{\sigma=\uparrow\downarrow} (\psi^{+}_{\mathbf{x},\sigma} f^{-}_{\mathbf{x},\sigma} + f^{+}_{\mathbf{x},\sigma}\psi^{-}_{\mathbf{x},\sigma}),$$

$$(j, A) = \int_{\mathbb{R}^3} \frac{d\mathbf{p}}{(2\pi)^3} \hat{A}_{\mathbf{p},\mu}\hat{j}_{\mathbf{p},\mu},$$

where $\hat{j}_{\mathbf{p},\mu} = \sum_{\sigma=\uparrow\downarrow} \int_{\mathbb{R}\times\mathcal{B}} \frac{d\mathbf{k}}{2\pi|\mathcal{B}|} \hat{\psi}^{+}_{\mathbf{k}+\mathbf{p},\sigma}\Gamma_{\mu}(\vec{k}, \vec{p})\hat{\psi}^{-}_{\mathbf{k},\sigma}$, in which $\Gamma_{\mu}(\vec{k}, \vec{p})$ are the *bare* vertex functions, namely: $\Gamma_0(\vec{k}, \vec{p}) = M(\vec{p})$, and, if $i = 1, 2$, $\Gamma_i(\vec{k}, \vec{p})$ are the two components of the (matrix-valued) vector $\vec{M}(\vec{k}, \vec{p})$ defined in (5) and following lines. In terms of these definitions, the correlations can be re-expressed as $S_2(\mathbf{x}, \mathbf{y}) = \frac{\partial^2\mathcal{W}}{\partial f^{+}_{\mathbf{x},\sigma}\partial f^{-}_{\mathbf{y},\sigma}}(0, 0)$, $K_{\mu\nu}(\mathbf{x}, \mathbf{y}) = \frac{\partial^2\mathcal{W}}{\partial j_{\mathbf{x},\mu}\partial j_{\mathbf{y},\nu}}(0, 0)$, and of suitable linear combinations of $G_{2,1;\mu}(\mathbf{x}, \mathbf{y}, \mathbf{z}) = \frac{\partial^3\mathcal{W}}{\partial A_{\mathbf{x},\mu}\partial f^{+}_{\mathbf{y},\sigma}\partial f^{-}_{\mathbf{z},\sigma}}(0, 0)$.

We now compute the generating function eq.(12) via a renormalized expansion, which is convergent uniformly close to (and even on) the critical line. Note that, on this line, the Grassmann integral has an infrared problem. In order to resolve and re-sum the corresponding singularities, we proceed in a multi-scale fashion. First of all, we distinguish the ultraviolet modes, corresponding to large values of the Matsubara frequency, from the infrared ones, by introducing two compactly supported cut-off functions, $\chi_{\pm}(\mathbf{k})$, supported in the vicinity of the Fermi points (more precisely, we let $\chi_{\pm}(\mathbf{k}) = \chi_0(\mathbf{k} - \mathbf{p}^{\pm}_F)$, where χ_0 is a smoothed out characteristic function of the ball of radius a_0, with a_0 equal to, say, $1/3$, and $\mathbf{p}^{\pm}_F = (0, \vec{p}^{\pm}_F)$) and by letting $\chi_{uv}(\mathbf{k}) = 1 - \sum_{\omega=\pm}\chi_{\omega}(\mathbf{k})$. We correspondingly split the propagator in its ultraviolet and infrared components:

$$g(\mathbf{x}, \mathbf{y}) = g^{(1)}(\mathbf{x}, \mathbf{y}) + \sum_{\omega=\pm} e^{-i\vec{p}^{\omega}_F(\vec{x}-\vec{y})} g^{(\leq 0)}_{\omega}(\mathbf{x}, \mathbf{y}) \qquad (14)$$

where $g^{(1)}(\mathbf{x}, \mathbf{y})$ and $g^{(\leq 0)}_{\omega}(\mathbf{x}, \mathbf{y})$ are defined in a way analogous to eq.(13), with $\hat{g}(\mathbf{k})$ replaced by $\chi_{uv}(\mathbf{k})\hat{g}(\mathbf{k})$ and by $\chi_0(\mathbf{k})\hat{g}(\mathbf{k} + \mathbf{p}^{\omega}_F)$, respectively. We then split the Grassmann field as a sum of two independent fields, with propagators $g^{(1)}$ and $g^{(\leq 0)}$:

$$\psi^{\pm}_{\mathbf{x},\sigma} = \psi^{\pm(1)}_{\mathbf{x},\sigma} + \sum_{\omega=\pm} e^{\pm i\vec{p}^{\omega}_F\vec{x}} \psi^{\pm(\leq 0)}_{\mathbf{x},\sigma,\omega}$$

and we rewrite the Grassmann Gaussian integration as the product of two independent Gaussians: $P(d\psi) = P(d\psi^{(\leq 0)})P(\psi^{(1)})$. By construction, the integration of the 'ultraviolet' field $\psi^{(1)}$ does not have any infrared singularity and, therefore, can be performed in a straightforward manner, thus allowing us to rewrite the generating function $\mathcal{W}(f, A)$ as the logarithm of

$$\frac{e^{\mathcal{W}^{(0)}(f,A)}}{\mathcal{N}_0} \int P(d\psi^{(\leq 0)}) e^{-V^{(0)}(\psi^{(\leq 0)}) + B^{(0)}(\psi^{(\leq 0)}, f, A)}, \qquad (15)$$

where $V^{(0)}$ and $B^{(0)}$ are, respectively, the effective potential and the effective source (which depend explicitly on, respectively, $\psi^{(\leq 0)}$ and $\psi^{(\leq 0)}, f, A$), $\mathcal{W}^{(0)}$ is independent of $\psi^{(\leq 0)}$ (and depends explicitly on f, A), and $\mathcal{N}_0 = \int P(d\psi^{(\leq 0)}) e^{-V^{(0)}(\psi^{(\leq 0)})}$. Both $V^{(0)}$ and $B^{(0)}$ are expressed as series of monomials in the ψ, f, A fields, whose kernels (given by the sum of all possible Feynman diagrams with fixed number and fixed location of

the external legs) are *analytic functions* of the interaction strength, for U sufficiently small. The proof of their analyticity is based on a determinant expansion and on a systematic use of the Gram-Hadamard bounds, see Ref.[29,35].

B. Symmetries

Before attacking the multi-scale integration of the infrared modes, we make a digression about the symmetry structure of the effective potential, and in particular of its local parts: the purpose is to classify the possible relevant and marginal coupling constants. In the case $t_2 = W = \mu = 0$ (standard graphene model) the lattice symmetries severely constrain the form of the quadratic terms in the effective potential: in particular, the interaction does not shift the chemical potential, nor does it generate a mass. In the general case ($W, t_2, \phi \neq 0$) the model is invariant under the following symmetry transformations (since they do not mix the spin indices, for notational convenience we temporarily drop the spin labels from the formulas). We discuss the symmetries in the *absence* of external fields, since we will use them only to infer the structure of the relevant and marginal contributions to the effective potential $V^{(0)}$. Once the structure of these terms is known, the structure of the marginal contributions to the effective source $B^{(0)}$ can be computed by using the Ward Identity (10).

(1) *Discrete rotations:* $\hat\psi^-_{\mathbf{k}} \to e^{i\vec k(\vec\delta_3-\vec\delta_1)n_-}\hat\psi^-_{T\mathbf{k}}$ and $\hat\psi^+_{\mathbf{k},\tau} \to \hat\psi^+_{T\mathbf{k},\tau}e^{-i\vec k(\vec\delta_3-\vec\delta_1)n_-}$, where, denoting the Pauli matrices by $\sigma_1,\sigma_2,\sigma_3$, $n_- = (1-\sigma_3)/2$, and $T\mathbf{k} = (k_0, e^{-i\frac{2\pi}{3}\sigma_2}\vec k)$ is the spatial rotation by $2\pi/3$ in the counter-clockwise direction.

(2) *Complex conjugation*: $\hat\psi^\pm_{\mathbf{k}} \to \hat\psi^\pm_{-\mathbf{k}}$, combined with $c \to c^*$, where c is a generic constant appearing in $P(d\psi)$ or in $V(\psi)$, and $\phi \to -\phi$.

(3) *Horizontal reflections*: $\hat\psi^-_{\mathbf{k}} \to \sigma_1\hat\psi^-_{R_h\mathbf{k}}$ and $\hat\psi^+_{\mathbf{k}} \to \hat\psi^+_{R_h\mathbf{k}}\sigma_1$, with $R_h\mathbf{k} = (k_0, -k_1, k_2)$, and $(W,\phi) \to (-W,-\phi)$.

(4) *Vertical reflections*: $\hat\psi^\pm_{\mathbf{k}} \to \hat\psi^\pm_{R_v\mathbf{k}}$, with $R_v\mathbf{k} = (k_0, k_1, -k_2)$, and $\phi \to -\phi$.

(5) *Particle-hole*: $\hat\psi^-_{\mathbf{k}} \to i\hat\psi^{+,T}_{P\mathbf{k},\tau}$, $\hat\psi^+_{\mathbf{k},\tau} \to i\hat\psi^{-,T}_{P\mathbf{k},\tau}$, with $P\mathbf{k} = (k_0, -k_1, -k_2)$, and $\phi \to -\phi$.

Note that at fixed W,ϕ the theory is invariant under the transformations (1), (2)+(4), and (2)+(5). In particular, these transformations leave the quadratic part $Q^{(0)}(\psi) = \sum_\sigma \int \frac{d\mathbf{k}}{(2\pi|\mathcal{B}|)}\hat\psi^+_{\mathbf{k},\sigma}\hat W_2(\mathbf{k})\hat\psi^-_{\mathbf{k},\sigma}$ of the effective potential $V^{(0)}(\psi)$ invariant. In terms of the kernel $\hat W_2(\mathbf{k})$ of the quadratic part, this means that:

$$\begin{aligned}\hat W_2(\mathbf{k}) &= e^{-i\vec k(\vec\delta_1-\vec\delta_2)n_-}\hat W_2(T^{-1}\mathbf{k})e^{i\vec k(\vec\delta_1-\vec\delta_2)n_-}\\ &= \hat W_2^*(-k_0,-k_1,k_2)\\ &= \hat W_2^\dagger(-k_0,k_1,k_2).\end{aligned} \tag{16}$$

As we will see in the next section, the value of $\hat W_2(\mathbf{k})$ and of its derivatives at the Fermi points defines the set of *effective coupling constants*. By using (16), we find, for $\omega = \pm$,

$$\begin{aligned}\hat W_2(\mathbf{p}^\omega_F) &= e^{-i\frac{2\pi}{3}\omega n_-}\hat W_2(\mathbf{p}^\omega_F)e^{i\frac{2\pi}{3}\omega n_-}\\ &= \hat W_2^*(\mathbf{p}^\omega_F) = \hat W_2^\dagger(\mathbf{p}^\omega_F),\end{aligned}$$

which implies that

$$\hat W_2(\mathbf{p}^\omega_F) = \nu_\omega + \delta_\omega\sigma_3, \tag{17}$$

for two *real* constants ν_ω and δ_ω.

If we derive (16) with respect to $\mathbf{k}$ and compute the result at $\mathbf{p}^\omega_F$, we find:

$$\begin{aligned}\partial_{\mathbf{k}}\hat W_2(\mathbf{p}^\omega_F) &= e^{-i\frac{2\pi}{3}\omega n_-}T\partial_{\mathbf{k}}\hat W_2(\mathbf{p}^\omega_F)e^{i\frac{2\pi}{3}\omega n_-}\\ &= (-R_v)\partial_{\mathbf{k}}\hat W_2^*(\mathbf{p}^\omega_F)\\ &= (-P)\partial_{\mathbf{k}}\hat W_2^\dagger(\mathbf{p}^\omega_F),\end{aligned} \tag{18}$$

where R_v (resp. P) is the diagonal matrix with diagonal elements $(1,1,-1)$ (resp. $(1,-1,-1)$). By using (18), it is straightforward to check that

$$\mathbf{k}'\partial_{\mathbf{k}}\hat W(\mathbf{p}^\omega_F) = \begin{pmatrix} -iz_{1,\omega}k_0 & -u_\omega(-ik'_1+\omega k'_2)\\ -u_\omega(ik'_1+\omega k'_2) & -iz_{2,\omega}k_0\end{pmatrix}, \tag{19}$$

where $\mathbf{k}' = \mathbf{k} - \mathbf{p}^\omega_F = (k_0, \vec{k'})$, and $u_\omega, z_{1,\omega}, z_{2,\omega}$ are *real* constants. In conclusion, for general values of W,ϕ, the linearization of $\hat W_2(\mathbf{k})$ at $\mathbf{p}^\omega_F$ is parametrized by 5 real constants, namely $\nu_\omega, \delta_\omega, u_\omega, z_{1,\omega}$ and $z_{2,\omega}$, the first two are relevant coupling constants, and the other three are marginal. Note that, in general, the values of these constants depend on ω (therefore, there are 5 of them at $\mathbf{p}^+_F$ and 5 more at $\mathbf{p}^-_F$). Note also that in general $z_{1,\omega} \neq z_{2,\omega}$, i.e., the wave function renormalization depends explicitly on the spinor index, an effect that can be checked explicitly in second order perturbation theory (see below), and cannot be explained purely in terms of the relativistic approximation of the model around the Fermi points.

Note that there are special points in the (W,ϕ) plane, for which the model has more symmetries, and where the number of independent couplings is smaller than in the general case.

In particular, if $W = \phi = 0$, the model is invariant under all the 5 symmetry transformations listed above, in which case it is straightforward to see that $\nu_\omega = \nu_{-\omega}$, $\delta_\omega = 0$, $u_\omega = u_{-\omega}$, and $z_{1,\omega} = z_{2,\omega} = z_{1,-\omega} = z_{2,-\omega}$. A similar discussion applies to the case $W = 0$, $\phi = \pi$.

Finally, if $\phi = \pi/2$, the model is invariant under the following additional symmetry transformation (see also Ref.[39]): $\hat\psi^-_{\mathbf{k}} \to -i\sigma_1\sigma_3\hat\psi^-_{-R_v\mathbf{k}}$, $\hat\psi^+_{\mathbf{k}} \to -i\hat\psi^+_{-R_v\mathbf{k}}\sigma_3\sigma_1$, which implies that

$$\hat W_2(\mathbf{k}) = -\sigma_3\sigma_1\hat W_2(-k_0,-k_1,k_2)\sigma_1\sigma_3,$$

so that, in particular, $\nu_\omega = 0$ and $z_{1,\omega} = z_{2,\omega}$. A similar discussion applies to $\pi = -\pi/2$.

C. Infrared integration

Let us now describe the integration of the infrared fields. We shall focus on the semi-metallic behavior of the system at, or very close to, a generic point of the critical line. Moreover, since we are interested in the behavior of the current-current correlations around $\mathbf{p}=\mathbf{0}$, we shall assume that the external field $\hat{A}_{\mathbf{p},\mu}$ is supported in the vicinity of the origin (in particular, we assume that it vanishes in the vicinity of $\mathbf{p}_F^{\omega}-\mathbf{p}_F^{-\omega}$, $\omega=\pm$).

By dimensional considerations, the quadratic terms in the effective action are *relevant*, and, the ones corresponding to the renormalization of the mass are of particular importance. The flow of the effective mass tends to diverge linearly under the RG iterations, which signals that, in general, the location of the critical lines is changed by the interaction. In order to construct a convergent expansion, we need to dress the mass, after which we determine the location of the renormalized critical lines, which is given by the condition that the dressed mass vanishes.

More in detail, we proceed as follows. We perform the integration of the infrared modes in (15) iteratively, by decomposing the fermionic fields as $\psi^{\pm(\leq 0)}_{\mathbf{x},\sigma,\omega}$ as $\psi^{\pm(\leq 0)}_{\mathbf{x},\sigma,\omega}=\sum_{h\leq 0}\psi^{\pm(h)}_{\mathbf{x},\sigma,\omega}$, where $\psi^{\pm(h)}_{\mathbf{x},\sigma,\omega}$ is a Grassmann field whose propagator is supported on the momenta $\mathbf{k}$ such that $|\mathbf{k}-\mathbf{p}_F^{\omega}|\sim 2^h$, and by integrating the fields $\psi^{(0)},\psi^{(-1)},\dots$ step by step. After the integration of the modes on scales $0,-1,\dots,h+1$, we rewrite the generating function $\mathcal{W}(f,A)$ as the logarithm of

$$\frac{e^{\mathcal{W}^{(h)}(f,A)}}{\mathcal{N}_h}\int P(d\psi^{(\leq h)})e^{-V^{(h)}(\psi^{(\leq h)})+B^{(h)}(\psi^{(\leq h)},f,A)}, \tag{20}$$

where $V^{(h)}$ and $B^{(h)}$ are, respectively, the effective potential and source terms, to be defined inductively in the following. Moreover, $P(d\psi^{(\leq h)})$ is the Grassmann Gaussian integration with propagator (diagonal with respect to the σ and ω indices)

$$\begin{aligned} g^{(\leq h)}_{\omega}(\mathbf{x},\mathbf{y}) &= \int P(d\psi^{(\leq h)})\psi^{-(\leq h)}_{\mathbf{x},\sigma,\omega}\psi^{+(\leq h)}_{\mathbf{y},\sigma,\omega} \\ &= \int \frac{d\mathbf{k}'}{2\pi|\mathcal{B}|}e^{-i\mathbf{k}'(\mathbf{x}-\mathbf{y})}\hat{g}^{(\leq h)}_{\omega}(\mathbf{k}'), \end{aligned}$$

where $\mathbf{k}'=(k_0,\vec{k}')$ and, letting $r_\omega(\vec{k}')=R(\vec{k}'+\vec{p}_F^{\,\omega})$, $s_\omega(\vec{k}')=-t_1[\Omega(\vec{k}'+\vec{p}_F^{\,\omega})-\frac{3}{2}(ik_1'+\omega k_2')]$ and $\chi_h(\mathbf{k}')=\chi_0(2^{-h}\mathbf{k}')$ (here χ_0 is the cutoff function defined a few lines before (14)),

$$\hat{g}^{(\leq h)}_{\omega}(\mathbf{k})=\chi_h(\mathbf{k}')\begin{pmatrix} a_{1,\omega,h}(\mathbf{k}') & b^*_{\omega,h}(\mathbf{k}') \\ b_{\omega,h}(\mathbf{k}') & a_{2,\omega,h}(\mathbf{k}')\end{pmatrix}^{-1}, \tag{21}$$

with

$$\begin{aligned} &a_{\rho,\omega,h}(\mathbf{k})=-ik_0Z_{\rho,\omega,h}+r_\omega(\vec{k}')+(-1)^{\rho-1}m_{\omega,h}(\vec{k}'),\\ &b_{\omega,h}(\mathbf{k}')=-v_{\omega,h}(ik_1'+\omega k_2')+s_\omega(\vec{k}')\ . \end{aligned} \tag{22}$$

in which $Z_{j,\omega,h}$, $m_{\omega,h}(\vec{k}')$ and $v_{\omega,h}$ are, respectively, the wave function renormalizations, the effective mass and effective velocities, to be defined inductively in the following. Their initial values are: $Z_{j,\omega,0}=1$, $m_{\omega,0}(\vec{k}')=m(\vec{k}'+\vec{p}_F^{\,\omega})$, $v_{\omega,0}=\frac{3}{2}t_1$.

In order to clarify the inductive definition of the effective potential, source, etc, we now describe the integration step at scale h. We start from (20), where $V^{(h)}(\psi)$ is a sum of even monomials in the ψ fields, whose kernels of order n are denoted by $W_n^{(h)}$ (for notational simplicity, we temporarily drop the space-time, spin, spinor and valley indices of the fermionic fields). Similarly, we denote the kernels of $B^{(h)}$ of order n in ψ, m in f and q in A, by $W_{n,m,q}$. The scaling dimension of the kernels W_n and $W_{n,m,q}$ is (see Ref.[29,35,36])

$$D=3-n-m-q, \tag{23}$$

with the convention that $D>0$ corresponds to relevant, $D=0$ to marginal, and $D<0$ to irrelevant operators. Note that the only relevant terms are those with $n+m=2$, and the only marginal terms are those with $n+m=2$ and $q=1$ (note that, by construction, $n+m$ is positive and even). In particular, the effective electron-electron interaction, corresponding to the case $n=4$ and $m=q=0$, is *irrelevant*.

In order to define a convergent renormalized expansion, we need to re-sum the relevant and marginal terms. For this purpose, we split $V^{(h)}$ and $B^{(h)}$ into their *local* and *irrelevant* parts (here, for simplicity, we spell out the definitions only in the $f=0$ case, the general case is treatable analogously, along the lines of, e.g., Sect.12 of Ref.[33], or Ref.[36]): $V^{(h)}=\mathcal{L}V^{(h)}+\mathcal{R}V^{(h)}$ and $B^{(h)}=\mathcal{L}B^{(h)}+\mathcal{R}B^{(h)}$, where (denoting the quadratic part of $V^{(h)}$ by $\sum_{\omega,\sigma}\int\frac{d\mathbf{k}'}{2\pi|\mathcal{B}|}\hat{\psi}^+_{\mathbf{k}',\sigma,\omega}\hat{W}^{(h)}_{2;\omega}(\mathbf{k}')\hat{\psi}^-_{\mathbf{k}',\sigma,\omega}$, and the part of $B^{(h)}$ of order $(2,0,1)$ in (ψ,f,A) by $\sum_{\omega,\sigma}\int\frac{d\mathbf{p}}{(2\pi)^3}\int\frac{d\mathbf{k}'}{2\pi|\mathcal{B}|}\hat{A}_{-\mathbf{p},\mu}\hat{\psi}^+_{\mathbf{k}'+\mathbf{p},\sigma,\omega}\hat{W}^{(h)}_{2,1;\mu,\omega}(\mathbf{k}',\mathbf{p})\hat{\psi}^-_{\mathbf{k}',\sigma,\omega}$)

$$\begin{aligned} \mathcal{L}V^{(h)}(\psi) &= \sum_{\omega=\pm}\sum_{\sigma=\uparrow\downarrow}\int\frac{d\mathbf{k}'}{2\pi|\mathcal{B}|}\times \\ &\times\hat{\psi}^+_{\mathbf{k}',\sigma,\omega}[\hat{W}^{(h)}_{2;\omega}(\mathbf{0})+\mathbf{k}'\partial_{\mathbf{k}'}\hat{W}^{(h)}_{2;\omega}(\mathbf{0})]\hat{\psi}^-_{\mathbf{k}',\sigma,\omega}, \\ \mathcal{L}B^{(h)}(\psi,0,A) &= \sum_{\omega=\pm}\sum_{\sigma=\uparrow\downarrow}\sum_{\mu=0}^{2}\int\frac{d\mathbf{p}}{(2\pi)^3}\int\frac{d\mathbf{k}'}{2\pi|\mathcal{B}|}\times \\ &\times\hat{A}_{\mathbf{p},\mu}\hat{\psi}^+_{\mathbf{k}'+\mathbf{p},\sigma,\omega}\hat{W}^{(h)}_{2,1;\mu,\omega}(\mathbf{0},\mathbf{0})\hat{\psi}^-_{\mathbf{k}',\sigma,\omega}. \end{aligned}$$

By the symmetries discussed in the previous section (see, in particular, (17) and (19))

$$\begin{aligned} \mathcal{L}V^{(h)}(\psi) = \sum_{\omega=\pm}\int\frac{d\mathbf{k}'}{2\pi|\mathcal{B}|}\Big[&2^h\nu_{\omega,h}\hat{\psi}^+_{\mathbf{k}',\sigma,\omega}\hat{\psi}^-_{\mathbf{k}',\sigma,\omega}+ \\ &+\hat{\psi}^+_{\mathbf{k}',\sigma,\omega}\begin{pmatrix}-iz_{1,\omega,h}k_0+\delta_{\omega,h} & -u_{\omega,h}(-ik_1'+\omega k_2')\\ -u_{\omega,h}(ik_1'+\omega k_2') & -iz_{2,\omega,h}k_0-\delta_{\omega,h}\end{pmatrix}\hat{\psi}^-_{\mathbf{k}',\sigma,\omega}\Big], \end{aligned} \tag{24}$$

where $\nu_{\omega,h},\delta_{\omega,h},z_{j,\omega,h},u_{\omega,h}$ are real constants. Moreover,

by using the Ward Identity (10), we find that

$$\mathcal{L}B^{(h)}(\psi,0,A)=\sum_{\omega=\pm}\sum_{\sigma=\uparrow\downarrow}\sum_{\mu=0}^{2}\int\frac{d\mathbf{p}}{(2\pi)^3}\int\frac{d\mathbf{k}'}{2\pi|\mathcal{B}|}\times$$
$$\times\hat{A}_{\mathbf{p},\mu}\hat{\psi}^{+}_{\mathbf{k}'+\mathbf{p},\sigma,\omega}\gamma_{\mu,\omega,h}\hat{\psi}^{-}_{\mathbf{k}',\sigma,\omega},\qquad(25)$$

where $\gamma_{0,\omega,h}=-\sum_{\rho=1}^{2}(Z_{\rho,\omega,h}+z_{\rho,\omega,h})n_\rho$, $\gamma_{1,\omega,h}=-(v_{\omega,h}+u_{\omega,h})\sigma_2$, and $\gamma_{2,\omega,h}=-\omega(v_{\omega,h}+u_{\omega,h})\sigma_1$, in which $n_\rho=(1+(-1)^{\rho-1}\sigma_3)/2$ and σ_i are the standard Pauli matrices.

Once the effective potential and source have been split into local and irrelevant parts, we combine the part of $\mathcal{L}V^{(h)}$ in the second line of (24) with the Gaussian integration $P(d\psi^{(\le h)})$, thus defining a dressed measure $\tilde{P}(d\psi^{(\le h)})$ whose propagator $\tilde{g}^{(\le h)}_{\omega}(\mathbf{x},\mathbf{y})$ is analogous to $g^{(\le h)}_{\omega}(\mathbf{x},\mathbf{y})$, with the only difference that the functions $a_{\rho,\omega,h}$, $b_{\omega,h}$ in (21)-(22) are replaced by

$$\tilde{a}_{\rho,\omega,h-1}(\mathbf{k})=-ik_0\tilde{Z}_{\rho,\omega,h-1}(\mathbf{k}')+r_\omega(\vec{k}')$$
$$+(-1)^{\rho-1}\tilde{m}_{\omega,h-1}(\mathbf{k}'),$$
$$\tilde{b}_{\omega,h-1}(\mathbf{k}')=-\tilde{v}_{\omega,h-1}(\mathbf{k}')(ik'_1+\omega k'_2)+s_\omega(\vec{k}'),$$

with

$$\tilde{Z}_{\rho,\omega,h-1}(\mathbf{k}')=Z_{\rho,\omega,h}+z_{\rho,\omega,h}\,\chi_h(\mathbf{k}'),$$
$$\tilde{m}_{\omega,h-1}(\mathbf{k}')=m_{\omega,h}(\vec{k}')+\delta_{\omega,h}\,\chi_h(\mathbf{k}'),$$
$$\tilde{v}_{\omega,h-1}(\mathbf{k}')=v_{\omega,h}+u_{\omega,h}\,\chi_h(\mathbf{k}').$$

Now, by rewriting the support function $\chi_h(\mathbf{k}')$ in the definition of $\tilde{g}^{(\le h)}_{\omega}(\mathbf{x},\mathbf{y})$ as $\chi_h(\mathbf{k}')=f_h(\mathbf{k}')+\chi_{h-1}(\mathbf{k}')$, we correspondingly rewrite: $\tilde{g}^{(\le h)}_{\omega}(\mathbf{x},\mathbf{y})=\tilde{g}^{(h)}_{\omega}(\mathbf{x},\mathbf{y})+g^{(\le h-1)}_{\omega}(\mathbf{x},\mathbf{y})$, where $g^{(\le h-1)}_{\omega}(\mathbf{x},\mathbf{y})$ is defined exactly as in (21)-(22), with h replaced by $h-1$, and $Z_{\rho,\omega,h-1},m_{\omega,h-1},v_{\omega,h-1}$ defined by the flow equations:

$$Z_{\rho,\omega,h-1}=Z_{\rho,\omega,h}+z_{\rho,\omega,h},$$
$$m_{\omega,h-1}(\vec{k}')=m_{\omega,h}(\vec{k}')+\delta_{\omega,h},\qquad(26)$$
$$v_{\omega,h-1}=v_{\omega,h}+u_{\omega,h}.$$

At this point, we integrate the fields on scale h, and define:

$$e^{-V^{(h-1)}(\psi)+B^{(h-1)}(\psi,f,A)+w^{(h)}(f,A)}=C_h\int\tilde{P}(d\psi^{(h)})\times$$
$$\times e^{-F^{(h)}_{\nu}(\psi^{(h)}+\psi)+\mathcal{R}V^{(h)}(\psi^{(h)}+\psi)+B^{(h)}(\psi^{(h)}+\psi,f,A)},$$

where $\tilde{P}(d\psi^{(h)})$ is the Gaussian integration with propagator $\tilde{g}^{(h)}_{\omega}$, $F^{(h)}_{\nu}(\psi)=\sum_\omega 2^h\nu_{\omega,h}\int\frac{d\mathbf{k}'}{2\pi|\mathcal{B}|}\hat{\psi}^{+}_{\mathbf{k}',\sigma,\omega}\hat{\psi}^{-}_{\mathbf{k}',\sigma,\omega}$, and $C_h^{-1}=\int\tilde{P}(d\psi^{(h)})e^{-F^{(h)}_{\nu}(\psi^{(h)})+\mathcal{R}V^{(h)}(\psi^{(h)})}$. Finally, letting $\mathcal{W}^{(h-1)}=\mathcal{W}^{(h)}+w^{(h)}$, we obtain the same expression as (20), with h replaced by $h-1$. This concludes the proof of the inductive step, corresponding to the integration of the fields on scale h.

The integration procedure goes on like this, as long as the two effective masses $m_{\pm,h}$ are small, as compared to 2^h. If we are not exactly at the 'graphene point' $W=\phi=0$, i.e., if we are close to, or at, any other point on the critical line but the origin, then after a while we reach a scale h_1 at which $\max_\omega|m_{\omega,h_1}|\equiv|m_{\omega_1,h_1}|\simeq 2^{h_1}$ (possibly, $h_1=0$, in the case that $\max_\omega|m_\omega|$ is of order 1, i.e., if W,ϕ are far enough from the graphene point). Note that, once we reach scale h_1, the field $\psi^{(\le h_1)}_{\mathbf{k}',\sigma,\omega_1}$ is massive 'on the right scale' 2^{h_1}. At that point, we integrate out the field $\psi^{(\le h_1)}_{\mathbf{k}',\sigma,\omega_1}$ in a single step, and we are left with a (chiral) theory, whose only dynamical degree of freedom is $\psi^{(\le h_1)}_{\mathbf{k}',\sigma,\omega_2}$, with $\omega_2=-\omega_1$.

From that scale on, we integrate $\psi^{(\le h_1)}_{\mathbf{k}',\sigma,\omega_2}=\sum_{h\le h_1}\psi^{(h)}_{\mathbf{k}',\sigma,\omega_2}$ in a multi-scale fashion, analogous to the one discussed above, with the important difference that only the running coupling constants corresponding to the valley index $\omega=\omega_2$ continue to flow. The multi-scale integration goes on until we reach a scale h_2 such that $|m_{\omega_2,h_2}|\simeq 2^{h_2}$, at which point we can integrate out the remaining degrees of freedom in a single step. The criticality condition, i.e., the condition that the system is on the (renormalized) critical line, corresponds to the condition that $h_2=-\infty$.

D. The flow of the running coupling constants

The multi-scale integration described in the previous section defines a flow for the effective chemical potential $\nu_{\omega,h}$, the effective mass $m_{\omega,h}=m_{\omega,h}(\vec{0})$, the effective wave function renormalization $Z_{\rho,\omega,h}$, and the effective Fermi velocity $v_{\omega,h}$. The flow of $m_{\omega,h},Z_{\rho,\omega,h}$ and $v_{\omega,h}$ is driven by eqs.(26), while

$$\nu_{\omega,h-1}=2\nu_{\omega,h}+\beta^{\nu}_{\omega,h},$$

where β^h_ν is the (ν-component of the) beta function, which is defined in terms of the sum of all the local quadratic contributions in renormalized perturbation theory, and should be thought of as a function of U and of the sequence of the effective coupling constants. Remember that the flow drives the effective couplings with both $\omega=+$ and $\omega=-$, up to the scale h_1; then the flow of the couplings with $\omega=\omega_1$ is stopped, and only the couplings with $\omega=\omega_2$ continue to flow until scale h_2 (possibly $h_2=-\infty$).

The multi-scale procedure is well defined, and the effective potentials are, step by step, given by *convergent* expansions, provided: (i) U is small enough, (ii) $\nu_{\omega,h}$ remain small for all scales, and (iii) $Z_{\rho,\omega,h},v_{\omega,h}$ remain close to their initial (bare) values, for all scales. Note that, in order for condition (ii) to be valid, we need to properly fix the initial condition on the chemical potential, as discussed in the following. In addition, note that, once that the flows of $Z_{\rho,\omega,h}$ and $v_{\omega,h}$ are controlled, then the marginal contributions to the effective source term $\mathcal{L}B^{(h)}(\psi,0,A)$ are automatically under control, thanks to (25) and following lines.

The key fact, which allows us to control the flow of the effective couplings, is that, since the electron-electron interaction is *irrelevant*, with scaling dimension $D = -1$ (cf. with (23)), then the scaling dimensions of all diagrams with at least one interaction vertex can be effectively improved by one, see Ref.[35]. In particular, $|\beta^\nu_{\omega,h}| \le c_\varepsilon |U| 2^{(1-\varepsilon)h}$, for any $\varepsilon > 0$ and a suitable constant $c_\varepsilon > 0$, and similarly for the beta functions of $Z_{\rho,\omega,h}$ and $v_{\omega,h}$. [The reason why we lose, in general, an ε in the decay exponent as $h \to -\infty$, is that we need to use a little bit of decay $2^{\varepsilon h}$ in order to sum over all diagrams and scales, see Ref.[35] for details.]

In order to guarantee that the flow of the chemical potential remains bounded, we fix the initial datum (via a fixed point theorem, such as the contraction mapping theorem) so that $\lim_{h\to-\infty} \nu_{\omega_2,h} = 0$, in the limit as $h_2 \to -\infty$. Thanks to the dimensional gain of $2^{(1-\varepsilon)h}$, due to the irrelevance of the interaction, we actually find that $\nu_{\omega_2,h}$ tends to zero as $h \to -\infty$ exponentially fast: $|\nu_{\omega_1,h}| \le$(const.)$|U| 2^{(1-\varepsilon)h}$. Once we imposed that $\nu_{\omega_2,h}$ remains bounded for all scales $h \le 0$, we can a posteriori check that $\nu_{\omega_1,h}$ is also bounded for all scales $h_1 \le h \le 0$: in fact, the beta function $\beta^\nu_{\omega_1,h}$, for $h \ge h_1$, can be rewritten as $\beta^\nu_{\omega_2,h} + [\beta^\nu_{\omega_1,h} - \beta^\nu_{\omega_2,h}]$, where the difference in square brackets can be straightforwardly shown to be proportional to m_{ω_1} [if all the masses $m_{\omega,h}$ were zero, then the model were symmetric under the exchange of ω in $-\omega$, as in Ref.[35], see also the section III B above; therefore, the difference $\beta^\nu_{\omega_1,h} - \beta^\nu_{\omega_2,h}$ between the contributions with different valley indices must be proportional to a mass term $|m_{\omega,h}|$, which is smaller than (const.)$|m_{\omega_1}|$]. Therefore, the flow of $\nu_{\omega_1,h}$, for $h \ge h_1$, remains close to the one of $\nu_{\omega_2,h}$ (which is uniformly bounded for all scales), up to terms that are proportional to m_{ω_1} and, therefore, are bounded by (const.)$|U||m_{\omega_1}| 2^{-h} 2^{(1-\varepsilon)h}$ (here 2^{-h} is the dimensional amplification factor arising from the scaling dimension $D = +1$ of the chemical potential terms, while $2^{(1-\varepsilon)h}$ is the dimensional gain coming from the irrelevance of the interaction). Recalling that $2^{h_1} \simeq |m_{\omega_1}|$, we find that $|\nu_{\omega_1,h}| \le$(const.)$|U| 2^{(1-\varepsilon)h}$, for all scales $h \ge h_1$.

Finally, once the chemical potential is fixed so that $|\nu_{\omega,h}| \le$(const.)$|U| 2^{(1-\varepsilon)h}$, we immediately infer that the beta functions of $Z_{\rho,\omega,h}$ and $v_{\omega,h}$ are bounded by (const.)$|U| 2^{(1-\varepsilon)h}$, as well: therefore, their flows converge exponentially fast, and the dressed values of $Z_{\rho,\omega,h}$ and $v_{\omega,h}$ are analytic functions of U, analytically close to their bare values.

E. Lowest order computations

The discussion in the previous section guarantees that, once the chemical potential is properly fixed, then the flows of the chemical potential, wave function renormalizations, and Fermi velocity converge exponentially fast. The values of the chemical potential, as well as of the dressed wave functional renormalizations, dressed Fermi velocity, and dressed critical lines are expressed in terms of convergent expansions (they are *analytic* functions of U), which are dominated by the first non trivial order in perturbation theory, provided U is not too large (note that the condition of convergence of the renormalized expansion is *uniform* in the gap, and is valid, in particular, *on the critical line*). The explicit lowest order contributions to the chemical potential ν, to the renormalized Fermi velocity $v_R \equiv v_{\omega_2,-\infty}$ and the wave function renormalizations $Z_{\rho,R} \equiv Z_{\rho,\omega_2,-\infty}$ on the renormalized critical line $h_2 = -\infty$ are the following:

1. Chemical potential:

$$\nu = -\frac{U^2}{2} \sum_{\rho=1}^{2} \int \frac{d\mathbf{k} d\mathbf{q}}{(2\pi|\mathcal{B}|)^2} \hat g_{\rho\rho}(\mathbf{k} + \mathbf{p}_F^{\omega_2}) \hat g_{\rho\rho}(\mathbf{q}) \hat g_{\rho\rho}(\mathbf{k}+\mathbf{q});$$

2. Fermi velocity:

$$v_R = \frac{3}{2} t_1 - iU^2 \int \frac{d\mathbf{k} d\mathbf{q}}{(2\pi|\mathcal{B}|)^2} \partial_{k_1} \hat g_{12}(\mathbf{k}+\mathbf{p}_F^{\omega_2}) \hat g_{12}(\mathbf{q}) \hat g_{21}(\mathbf{k}+\mathbf{q}); \tag{27}$$

3. Wave function renormalizations:

$$Z_{\rho,R} = 1 + iU^2 \int \frac{d\mathbf{k} d\mathbf{q}}{(2\pi|\mathcal{B}|)^2} \partial_{k_0} \hat g_{\rho\rho}(\mathbf{k}+\mathbf{p}_F^{\omega_2}) \hat g_{\rho\rho}(\mathbf{q}) \hat g_{\rho\rho}(\mathbf{k}+\mathbf{q}). \tag{28}$$

Moreover, the equation for the critical line $h_2 = -\infty$ reads:

$$m_{\omega_2} = \frac{U}{2} \int \frac{d\vec k}{|\mathcal{B}|} \frac{m(\vec k)}{\sqrt{m^2(\vec k) + t_1^2 |\Omega(\vec k)|^2}} \,,$$

where m_ω, $m(\vec k)$ and $\Omega(\vec k)$ where defined after (11). This is a fixed point equation for m_{ω_2}, whose solution leads to the plot in Fig.1.

Note that, as discussed in Sect.III B, there is no symmetry reason why $Z_{1,R}$ should be equal to $Z_{2,R}$. Actually, an explicit computation shows that $Z_{1,R} - Z_{2,R}$ is different from zero along the critical line, unless we are at one of the highly symmetric points $\phi = 0$ or $\phi = \pi/2$, see Fig.2.

IV. QUANTIZATION OF THE CONDUCTIVITY

In this section we compute the jump discontinuity of the Hall conductivity across the critical line, as well as the value of the longitudinal conductivity on the same line, and prove a universality result for both of them, i.e., we prove that their values are quantized and exactly independent of the interaction strength U. Note that this fact is highly non-trivial, due to the unusual renormalization of the Fermi velocity and of the wave function renormalizations, which depends explicitly on the spinor index and break the asymptotic relativistic invariance of the

propagator: the cancellations behind universality need to take lattice (and, therefore, RG-irrelevant) effects into account, and do not follow from asymptotic relativistic computations.

We stress that our result is exact at all orders of the (convergent, renormalized) expansion for the conductivity. One key ingredient used in the proof is the lattice Ward Identity (9), which is rigorously valid (without any sub-leading correction), thanks to the exact lattice symmetries and the fact that the correlations appearing at both sides can be computed in terms of convergent expansions, following from the multi-scale construction described above.

A. Quantization of the Hall conductivity across the critical line

Here we compute the universal jump discontinuity of the Hall conductivity across the renormalized critical line. We assume *not* to be at the graphene point $W = \phi = 0$, the computation in that special, highly symmetric, case is analogous to the general case. Therefore, the goal is to compute:

$$\Delta = \lim_{m_R\to 0^+} \sigma_{12} - \lim_{m_R\to 0^-} \sigma_{12} \,,$$

where $m_R \equiv m_{\omega_2,h_2}$ is the mass gap of the dressed propagator. The condition that we are not at the graphene point means that m_{ω_1,h_1} should be kept finite as $m_R \to 0$. Using the definition (8), as well as the fact that $\hat K_{ij}(\mathbf{p})$ is differentiable in $\mathbf{p}$ outside the critical line, we can rewrite

$$\Delta = -\frac{1}{A}\Big[\lim_{m_R\to 0^+} \partial_{p_0}\hat K_{12}(\mathbf{0}) - \lim_{m_R\to 0^-} \partial_{p_0}\hat K_{12}(\mathbf{0})\Big].$$

The interacting current-current correlation can be computed via the multiscale renormalized expansion discussed in Sect.III C: in particular, proceeding as in Ref.[36], among the contributions to $\hat K_{ij}$ we can distinguish the dominant contribution, coming from the 'dressed bubble', from the sub-dominant one, which is the sum over all the renormalized diagram with at least one interaction term. Thanks to the irrelevance of the interaction, these sub-dominant diagrams have a dimensional gain (of order 2^h on scale h), which makes the corresponding contribution to $\hat K_{ij}(\mathbf{p})$ *differentiable* at $\mathbf{p} = \mathbf{0}$, in the limit $m_R \to 0$. In particular, they give zero contribution to Δ.

The dominant contribution to $\hat K_{ij}(\mathbf{p})$ (i.e., the 'dressed bubble') is

$$\hat K^{dom}_{ij}(\mathbf{p}) = -2\int \frac{d\mathbf{k}}{2\pi|\mathcal{B}|}\mathrm{Tr}\big\{\hat S_2(\mathbf{k})\hat\Gamma_i(\mathbf{k},\mathbf{p})\times \\ \times \hat S_2(\mathbf{k}+\mathbf{p})\hat\Gamma_j(\mathbf{k}+\mathbf{p},-\mathbf{p})\big\},$$

where $\hat\Gamma_j$ is the vertex function defined in (7), and the factor 2 in front of the integral takes into account the spin degrees of freedom. Note that both $\hat S_2(\mathbf{k})$ and $\hat\Gamma_i(\mathbf{k},\mathbf{p})$ are *infinite* convergent renormalized series, depending on the details of the microscopic model.

The finite contribution to the jump-discontinuity of $\partial_{p_0}\hat K_{12}(\mathbf{0})$ across $m_R = 0$ comes from the integration over $\mathbf{k}$ in the vicinity of $\mathbf{p}_F^{\omega_2}$, since the rest is continuous as $m_R \to 0$. For the same reason, for the purpose of computing Δ, we can replace $\hat\Gamma_i(\mathbf{k},\mathbf{p})$ by $\hat\Gamma_i(\mathbf{p}_F^{\omega_2}) = \hat\Gamma_i(\mathbf{p}_F^{\omega_2},\mathbf{0})$, and $\hat S_2(\mathbf{k})$ by its linearization $\bar S(\mathbf{k}')$ at $\mathbf{p}_F^{\omega_2}$,

$$\bar S(\mathbf{k}') = \begin{pmatrix} -ik_0 Z_{1,R} + m_R & -v_R(-ik'_1 + \omega_2 k'_2) \\ -v_R(ik'_1 + \omega_2 k'_2) & -ik_0 Z_{2,R} - m_R \end{pmatrix}^{-1}, \tag{29}$$

where $Z_{\rho,R}$ and v_R are *analytic* functions of U, for U small, whose expansions at second order in U are given explicitly by (27)-(28). Recall that, a priori, $\hat\Gamma_i(\mathbf{p}_F^{\omega_2})$ are complicated infinite series in U. In particular, if one did not use the Ward identity (10), a direct computation of the jump-discontinuity, starting from the expression of the dressed bubble and from the Feynman rules for the generic term in the renormalized expansions for $Z_{\rho,R}$, v_R and $\hat\Gamma(\mathbf{p}_F^{\omega})$ would be hopeless.

The key fact is that, thanks to the Ward Identity (10),

$$\hat\Gamma_i(\mathbf{p}_F^{\omega_2}) = \partial_{k'_i}\bar S^{-1}(\mathbf{0})$$

that is, $\hat\Gamma_1(\mathbf{p}_F^{\omega_2}) = -v_R\sigma_2$ and $\hat\Gamma_2(\mathbf{p}_F^{\omega_2}) = -\omega_2 v_R\sigma_1$. Therefore, using the fact that $A|\mathcal{B}| = 4\pi^2$,

$$\Delta = \Big(\lim_{m_R\to 0^+} - \lim_{m_R\to 0^-}\Big)\int_{|\vec k'|\le\varepsilon}\frac{d\vec k'}{2\pi^2}\int_{\mathbb{R}}\frac{dk_0}{2\pi}\times \\ \times\mathrm{Tr}\big\{\bar S(\mathbf{k}')\partial_1\bar S^{-1}(\mathbf{0})\partial_0\bar S(\mathbf{k}')\partial_2\bar S^{-1}(\mathbf{0})\big\}, \tag{30}$$

where ε is a small, arbitrary, constant. Using the identity $\partial_0\bar S(\mathbf{k}')\bar S^{-1}(\mathbf{k}') = -\bar S(\mathbf{k}')\partial_0\bar S^{-1}(\mathbf{k}')$, and replacing $\bar S(\mathbf{k}')\partial_0\bar S^{-1}(\mathbf{k}')$ by $\bar S(\mathbf{k}')\partial_0\bar S^{-1}(\mathbf{0})$ (which is allowed, for the purpose of computing Δ, simply because the difference is continuous at $m_R = 0$), we can further rewrite Δ as

$$\Delta = -\Big(\lim_{m_R\to 0^+} - \lim_{m_R\to 0^-}\Big)\int_{|\vec k'|\le\varepsilon}\frac{d\vec k'}{2\pi^2}\int_{\mathbb{R}}\frac{dk_0}{2\pi}\times \\ \times\mathrm{Tr}\big\{\bar S(\mathbf{k}')\partial_1\bar S^{-1}(\mathbf{0})\bar S(\mathbf{k}')\partial_0\bar S^{-1}(\mathbf{0})\bar S(\mathbf{k}')\partial_2\bar S^{-1}(\mathbf{0})\big\}.$$

The integral over k_0 can be computed explicitly and, after a straightforward computation, we get

$$\Delta = \frac{\omega_2 v_R^2}{4\pi^2}\frac{Z_{1,R}+Z_{2,R}}{(Z_{1,R}Z_{2,R})^2}\lim_{m_R\to 0^+} m_R \times \\ \times\int_{|\vec k'|\le\varepsilon} d\vec k'\Big[\frac{m_R^2}{4}\big(\frac{1}{Z_{1,R}}+\frac{1}{Z_{2,R}}\big)^2 + \frac{v_R^2|\vec k'|^2}{Z_{1,R}Z_{2,R}}\Big]^{-3/2}.$$

Now, the integral over $\vec k'$ is elementary, and its computation makes apparent the exact cancellation of all the constants v_R, $Z_{1.R}$, $Z_{2,R}$. The final result is

$$\Delta = \omega_2/\pi,$$

as desired. At the graphene point, the analogous computation gives twice the same value, because of an extra factor 2 coming from the valley degeneracy.

B. Quantization of the longitudinal conductivity on the critical line

A similar discussion as the one in the previous subsection can be repeated for the *longitudinal* conductivity on the renormalized critical line. The point here, as compared to the computation of Δ in the previous subsection, is to take first the limit $m_R \to 0$, and then $p_0 \to 0^+$ (see the definition of conductivity, eq.(8)). Once again, we assume for definiteness not to be exactly at the graphene point (a similar discussion applies there, too).

Note that, by the very definition of current-current correlations, $\hat{K}_{\rho\rho}(p_0, \vec{0})$ is *even* in p_0. Therefore, all the contributions to $\hat{K}_{\rho\rho}(p_0, \vec{0})$ that are differentiable in p_0 give zero contribution to the longitudinal conductivity on the critical line. By repeating a discussion analogous to the one that lead us to (30), for the purpose of computing the longitudinal conductivity on the critical line, we can: (i) replace the full current-current correlation by its dominant contribution (from the 'dressed bubble'); (ii) restrict the integration over the loop momenta in the vicinity of $\mathbf{p}_F^{\omega_2}$; (iii) linearize the propagators and vertex functions around $\mathbf{p}_F^{\omega_2}$. After these replacements, we get (denoting the value of the longitudinal conductivity on the critical line by $\sigma^{cr}_{\rho\rho}$):

$$\sigma^{cr}_{\rho\rho} = \frac{2}{A} \lim_{p_0\to 0^+} \frac{1}{p_0} \int_{|\vec{k}'|\le\varepsilon} \frac{d\vec{k}'}{|\mathcal{B}|} \int_{\mathbb{R}} \frac{dk_0}{2\pi} \big[F(\mathbf{k}', p_0) - F(\mathbf{k}', 0)\big],$$

with

$$F(\mathbf{k}', p_0) = \mathrm{Tr}\Big\{ \bar{S}_0(\mathbf{k}') \partial_\rho \bar{S}_0^{-1}(\mathbf{0}) \bar{S}_0(k_0 + p_0, \vec{k}') \partial_\rho \bar{S}_0^{-1}(\mathbf{0}) \Big\}$$

and $\bar{S}_0(\mathbf{k}')$ is the linearized propagator (29) computed at $m_R = 0$.

By computing the integral over k_0 explicitly, and letting $\kappa = v_R/\sqrt{Z_{1,R} Z_{2,R}}$, we get

$$\sigma^{cr}_{\rho\rho} = \frac{1}{2\pi} \lim_{p_0\to 0^+} \int_0^{\kappa\varepsilon} \frac{p_0}{p_0^2 + 4x^2}\, dx = \frac{1}{8}.$$

Also in this case, the analogous computation performed at the graphene point gives twice the same value, in agreement with the result of Ref.[36].

V. CONCLUSIONS

We studied the Haldane-Hubbard model by rigorous Renormalization Group techniques. Our analysis predicts that the critical lines separating the distinct topological phases are modified non-trivially by the on-site interactions, and rules out the presence of new interaction-induced topological phases in the vicinity of the phase boundaries. Such predictions may be verified experimentally in optical lattice realizations of the system[11], where the on-site interaction can be produced and tuned by means of Feshbach resonances. Concerning numerical simulations, our results agree with[16,26].

The interaction affects the relativistic structure of the two-point function by non-universal renormalizatized coefficients, which differ from those obtained by approximate treatments of the system based on the effective Dirac theory. In particular, we find that there are two different wave function renormalizations, one for each pseudo-spin index. Despite the non-universal renormalization of the two-point function and of the vertex functions, lattice Ward identities guarantee the quantization and the universality of the conductivity matrix at the critical line.

Our results require that the interaction is weak and short-range; instead, different features are expected in the presence of long-range interactions. For instance, it is known that, at the graphene point, long-range interactions have a dramatic effect on several physical properties[40,41], in particular, on the optical conductivity[42–48]. We expect such effects to have profound implications for the Haldane-Hubbard model, especially in the proximity of the critical lines separating the different topological phases. We plan to investigate this in a future work.

The work of A.G. has been carried out thanks to the support of the A*MIDEX project Hypathie (no ANR-11-IDEX-0001-02) funded by the "Investissements d'Avenir" 25 French Government program, managed by the French National Research Agency (ANR), and by a C.N.R.S. visiting professorship spent at the University of Lyon-1. The work of M.P. has been carried out thanks to the support of the NCCR SwissMap.

Appendix A: Peierls' substitution and the bare vertex functions

In order to define the current, we couple the electron gas to an external vector potential $\vec{A}$, by multiplying the hopping strength from $\vec{y}$ to $\vec{x}$ by an extra phase factor $e^{i(\vec{y}-\vec{x})\int_0^1 \vec{A}((1-s)\vec{x}+s\vec{y})ds}$ (Peierls' substitution). We denote by $H(\vec{A})$ the modified Hamiltonian, and let the (paramagnetic) current be $J_{\vec{p},i} = \delta H(\vec{A})/\delta \hat{A}_{\vec{p},i}\big|_{\vec{A}=\vec{0}}$, where $i = 1, 2$ label the two (orthogonal) coordinate directions $\hat{e}_1 = (1, 0)$ and $\hat{e}_2 = (0, 1)$. An explicit computation leads to (5), with $\vec{M}(\vec{k}, \vec{p}) = \begin{pmatrix} \vec{M}_{11}(\vec{k}, \vec{p}) & \vec{M}_{12}(\vec{k}, \vec{p}) \\ \vec{M}_{21}(\vec{k}, \vec{p}) & \vec{M}_{22}(\vec{k}, \vec{p}) \end{pmatrix}$ and, defining $\eta_x = (e^{-ix} - 1)/(-ix)$,

$$\vec{M}_{11}(\vec{k}, \vec{p}) = -it_2 \sum_{j=1}^{3} \sum_{\alpha=\pm} \alpha \vec{\gamma}_j \eta_{\alpha\vec{p}\cdot\vec{\gamma}_j} e^{i\alpha(\phi - \vec{k}\cdot\vec{\gamma}_j)},$$

$$\vec{M}_{12}(\vec{k}, \vec{p}) = -it_1 \sum_{j=1}^{3} \vec{\delta}_j \eta_{\vec{p}\cdot\vec{\delta}_j} e^{-i\vec{k}(\vec{\delta}_j - \vec{\delta}_1)}\ ,$$

$\vec{M}_{21}(\vec{k},\vec{p}) = -\vec{M}_{12}(-\vec{k}-\vec{p},\vec{p})$ and $\vec{M}_{22}(\vec{k},\vec{p}) = -e^{-i\vec{p}\cdot\vec{\delta}_1}\vec{M}_{11}(-\vec{k},-\vec{p})$.

Appendix B: Details of the numerical computations

In this appendix, we discuss some of the details of the numerical computations from which Figs.1-2 were produced. The program used to carry them out is available online[49], has been named `hhtop`, and is released under an Apache license. The source code includes a documentation file, in which the computations are described in greater detail.

1. Integration scheme

The numerical computations carried out in this work involve numerical evaluations of integrals. The algorithm that was used to carry these out is based on *Gauss-Legendre* quadratures, by which, given an integer $N > 1$, an integral is approximated by a discrete sum with N terms:

$$\int_{-1}^{1} dx\ f(x) = \sum_{i=1}^{N} w_i f(x_i) + \mathfrak{R}_N \tag{B1}$$

where $x_1 < \cdots < x_N$ are the roots of the N-th Legendre polynomial P_N, and

$$w_i := \frac{2}{(1-x_i^2)P_N'(x_i)}. \tag{B2}$$

If f is an analytic function, then one can show that the remainder $\mathfrak{R}_N$ decays exponentially in N. However, in order to compute the difference of the wave-function renormalizations, we need to compute the integral of an integrand that, instead of being analytic, is a class-2 Gevrey function (a class-s Gevrey function is a $\mathcal{C}^\infty$ function whose n-th derivative is bounded by $(\text{const.})^n(n!)^s$, so that analytic functions are class-1 Gevrey functions). The remainder $\mathfrak{R}_N$ can be shown to be bounded, if f is a class-s Gevrey function with $s \geq 1$ and N is large enough (independently of f and s), by

$$|\mathfrak{R}_N| \leqslant c_0 c_1^{s-1}(2N)^{1-\frac{1}{s}} e^{-b(2N)^{\frac{1}{s}}} s! \tag{B3}$$

for some $c_0, c_1, b > 0$, that only depend on f. For a proof of this statement, see lemma A3.1 in the documentation of `hhtop`[49]. In short, this estimate is obtained by expanding f in Chebyshev polynomials, and using a theorem of A.C. Curtis and P. Rabinowitz[50] that shows that, if f is the j-th Chebyshev polynomial, then $\mathfrak{R}_N$ is bounded uniformly in j. The decay of the coefficients of the Chebyshev expansion of class-s Gevrey polynomials allows us to conclude.

2. First-order renormalization of the critical line

At first order in U, the correction $F_{\pm,R}(U,W,\phi)$ appearing in (2) is

$$F_\pm = \frac{U}{2}\int_{\mathcal{B}} \frac{d\vec{k}}{|\mathcal{B}|}\ \frac{m(\vec{k})}{\sqrt{m^2(\vec{k}) + t_1^2|\Omega(\vec{k})|^2}}. \tag{B4}$$

There is a single, minor, pitfall in the numerical evaluation of $F_\pm$: we wish to use Gauss-Legendre quadratures (see App.B 1) to carry out the computation, but the integrand in (B4) is not smooth: indeed, if $W = \pm 3\sqrt{3}t_2 \sin\phi$, then its second derivative diverges at $p_F^\pm$ due to the divergence of the derivative of $\sqrt{\cdot}$. However, by switching to polar coordinates $\vec{k} = p_F^\pm + \rho(\cos\theta, \sin\theta)$, this singularities is regularized, that is, the integrand becomes a smooth function of ρ and θ. At this point, there is yet another danger to avoid: while the integrand is smooth, the upper bound of the integral over ρ is a function of θ, which is, due to the rhombic shape of $\mathcal{B}$, only smooth by parts. The integral over θ must, therefore, be split into parts in which the bounds of the integral over ρ are smooth. This can be done very easily using the $\frac{2\pi}{3}$ rotation symmetry. Once both of these traps have been thwarted, Gauss-Legendre quadratures yield very accurate results.

In order to compute the correction to the critical line, we solve

$$W \pm 3\sqrt{3}t_2 \sin\phi - F_\pm(\phi, W) = 0 \tag{B5}$$

for W and ϕ. For the sake of clarity, we have made the (ϕ, W) dependence of $F_\pm$ explicit. To solve (B5), we fix ϕ, and use a Newton algorithm to compute the critical value of W: we set $W_0 = \mp 3\sqrt{3}t_2 \sin\phi$, and compute

$$W_{n+1} = W_n - \frac{W_n \pm 3\sqrt{3}t_2 \sin\phi - F_\pm(\phi, W_n)}{1 - \partial_W F_\pm(\phi, W_n)}. \tag{B6}$$

Provided W_0 is not too far from the solution of (B5), W_n converges *quadratically* (i.e. $|W_{n+1} - W_n| \leq (\text{const.})|W_n - W_{n-1}|^2$, in which the constant depends on the supremum of $\partial_W^2 F_\pm$, which is bounded) to the solution of (B5).

3. Second-order wave function renormalization

At second order in U, $Z_{1,R} - Z_{2,R}$ is

$$U^2(z_1 - z_2) = U^2 i\left(\partial_{k_0} s_1|_{k_0=0} - \partial_{k_0} s_2|_{k_0=0}\right) \tag{B7}$$

where

$$s_i := \int_{\mathcal{B}} \frac{d\vec{p}d\vec{q}}{|\mathcal{B}|^2} \int_{-\infty}^{\infty} \frac{dp_0 dq_0}{(2\pi)^2} \hat{g}_{i,i}(\mathbf{p})\hat{g}_{i,i}(\mathbf{q})\hat{g}_{i,i}(\mathbf{p}+\mathbf{q}-\mathbf{k}_F^\omega). \tag{B8}$$

The computation is carried out on the critical line, that is, when $W = -\omega 3\sqrt{3}t_2 \sin\phi$. The integrals over p_0 and q_0 can be carried out explicitly:

$$z_1 - z_2 = \int_{\mathcal{B}} \frac{d\vec{p}d\vec{q}}{|\mathcal{B}|^2} \cdot \cdot \left(\frac{(\xi_p + \xi_q + \xi_F)(\frac{m_p}{\xi_p} + \frac{m_q}{\xi_q} - \frac{m_F}{\xi_F} - \frac{m_p m_q m_F}{\xi_p \xi_q \xi_F})Z}{(Z^2 - (\xi_p + \xi_q + \xi_F)^2)^2} \right) \tag{B9}$$

where, using the definitions of $m(\vec{k})$, $R(\vec{k})$ and $\Omega(\vec{k})$ after (11) and after (13), $m_p \equiv m(\vec{p})$, $m_q \equiv m(\vec{q})$, $m_F \equiv m(\vec{p}+\vec{q}-\vec{p}^{\omega}_F)$, $\xi(\vec{k}) := \sqrt{m(\vec{k}) + t_1^2|\Omega(\vec{k})|^2}$, $Z := R(\vec{p}) + R(\vec{q}) - R(\vec{p}+\vec{q}-\vec{p}^{\omega}_F)$ and $\xi_p \equiv \xi(\vec{p})$, $\xi_q \equiv \xi(\vec{q})$, $\xi_F \equiv \xi(\vec{p}+\vec{q}-\vec{p}^{\omega}_F)$.

The numerical evaluation of the integral in (B9) involves a similar difficulty to that in (B4): the integrand has divergent derivatives if any of the following conditions hold: $\vec{p} = \vec{p}^{\omega}_F$, $\vec{q} = \vec{p}^{\omega}_F$ or $\vec{p} + \vec{q} = 2\vec{p}^{\omega}_F$. These singularities cannot be regularized by changing $\vec{p}$ and $\vec{q}$ to polar coordinates, since ξ_F is a singular function of the polar coordinates of $\vec{p}$ and $\vec{q}$ (due to the fact that it behaves, asymptotically, as $\vec{p}-\vec{q}$ approaches $2\vec{p}^{\omega}_F$, as $|\vec{p}+\vec{q}-2\vec{p}^{\omega}_F|$, which has divergent second derivatives). However, there are coordinates, which we call *sunrise coordinates* (since s_i is the value of the so-called *sunrise* Feynman diagram), which regularize these singularities. Their expression is rather long, and will not be expounded here; the interested reader is invited to consult the documentation file bundled with the source code of `hhtop`[49]. Once written in terms of the sunrise coordinates, the integral in (B9) can be computed using Gauss-Legendre quadratures very accurately.

[1] M. Z. Hasan and C. L. Kane, Rev. Mod. Phys. 82, 3045 (2010).
[2] X.-L. Qi and S.-C. Zhang, Rev. Mod. Phys. 83, 1057 (2011).
[3] J. E. Avron, R. Seiler and B. Simon, Phys. Rev. Lett. 51, 51 (1983).
[4] D. J. Thouless, M. Kohmoto, M. P. Nightingale and M. den Nijs, Phys. Rev. Lett. 49, 405 (1982).
[5] C. L. Kane and E. J. Mele, Z_2 Topological order and the quantum spin Hall effect, Phys. Rev. Lett. 95, 146802 (2005).
[6] A. Kitaev, AIP Conf. Proc. 1134(1), 22-30 (2009).
[7] D.S. Freed and G.W. Moore, Ann. Henri Poincaré 14, 1927-2023 (2013).
[8] D. Fiorenza, D. Monaco and G. Panati, Comm. Math. Phys., in press (arxiv:1408.1030).
[9] D. Carpentier, P. Delplace, M. Fruchart and K. Gawedzki, Phys. Rev. Lett. 114, 106806 (2015); D. Carpentier et al., Nucl. Phys. B 896, 779-834 (2015).
[10] F. D. M. Haldane, Phys. Rev. Lett. 61, 2015 (1988).
[11] G. Jotzu et al., Nature 515, 237 (2014).
[12] J. He et.al, Phys. Rev. B 84, 035127 (2011).
[13] J. He, Y. Liang, S.-P. Kou, Phys. Rev. B 85, 205107 (2012).
[14] Y.-X. Zhu, J. He, C.-L. Zang, Y. Liang, and S.-P. Kou, Journal of Physics: Condensed Matter 26, 175601 (2014).
[15] Y.-J. Wu, N. Li, and S.-P. Kou, The European Physical Journal B 88, 255 (2015).
[16] D. Prychynenko and S. Huber, Physica B: Condensed Matter 481, 53-58 (2016).
[17] W. Zheng, H. Shen, Z. Wang and H. Zhai, Phys. Rev. B 91, 161107(R)
[18] Z.-L. Gu, K. Li and J.-X. Li, `arXiv:1512.05118`.
[19] J. Wu, J. P. L. Faye, D. Senechal and J. Maciejko, Phys. Rev. B 93, 075131 (2016).
[20] J. He, S.-P. Kou, Y. Liang and S. Feng, Phys. Rev. B 83, 205116 (2011).
[21] J. Maciejko and A. Ruegg, Phys. Rev. B 88, 241101(R) (2013).
[22] C. N. Varney, K. Sun, M. Rigol and V. Galitski, Phys. Rev. B 82, 115125 (2010).
[23] C. N. Varney, K. Sun, M. Rigol, and V. Galitski, Phys. Rev. B 84, 241105(R) (2011).
[24] Y.-F. Wang, Z.-C. Gu, C.-D. Gong and D. N. Sheng, Phys. Rev. Lett. 107, 146803 (2011).
[25] I. Vasic, A. Petrescu, K. Le Hur and W. Hofstetter, Phys. Rev. B 91, 094502 (2015).
[26] T. I. Vanhala et al., `arXiv:1512.08804`.
[27] S. Coleman and B. Hill, Phys. Lett. 159B, 184 (1985).
[28] K. Ishikawa and T. Matsuyama, Z. Phys C 33, 41 (1986).
[29] A. Giuliani, V. Mastropietro and M. Porta, Comm. Math. Phys., in press (arXiv:1511.04047).
[30] G. Benfatto and G. Gallavotti, Jour. Stat. Phys. 59, 541-664 (1990).
[31] G. Benfatto and G. Gallavotti, Renormalization Group, Princeton University Press, 1995.
[32] V. Mastropietro, Non-perturbative Renormalization, World Scientific, 2008.
[33] G. Gentile and V. Mastropietro, Phys. Rep. 352, 273 (2001).
[34] A. Amaricci et al., Phys. Rev. Lett. 114, 185701 (2015); and Phys. Rev. B, in press (arXiv:1603.04263).
[35] A. Giuliani and V. Mastropietro, Comm. Math. Phys. 293, 301 (2010).
[36] A. Giuliani, V. Mastropietro and M. Porta, Phys. Rev. B 83, 195401 (2011); and Comm. Math. Phys. 311, 317 (2012).
[37] In formulæ, $\mathcal{B} = \{\vec{k} : \vec{k} = a_1\vec{\ell}^*_1 + a_2\vec{\ell}^*_2,\ a_i \in [0,1)\}$, where $\vec{\ell}^*_{1,2} = \frac{2\pi}{3}(1, \mp\sqrt{3})$ are the basis vectors of the reciprocal lattice Λ^*_A.
[38] The definition of $S_2(\mathbf{x},\mathbf{y})$ is meant as the limit as $\beta \to \infty$ of $S_2^{\beta}(\mathbf{x},\mathbf{y})$, which is the anti-periodic extension in x_0 and y_0 (of anti-period β in both variables) of $\langle \mathbf{T}\, \Psi^-_{\vec{x},\sigma}(x_0)\Psi^+_{\vec{y},\sigma}(y_0)\rangle_{\beta}$, with $x_0, y_0 \in [0,\beta)$. At equal times, we let $\mathbf{T}\, \Psi^-_{\vec{x},\sigma}(x_0)\Psi^+_{\vec{y},\sigma}(x_0) = -\Psi^+_{\vec{y},\sigma}(x_0)\Psi^-_{\vec{x},\sigma}(x_0)$. The same conventions hold for the mixed current-current and current-field correlations introduced below.
[39] Y. Zhang, Z. Xu, S. Zhang, `arXiv:1511.03833`.
[40] J. González, F. Guinea and M.A.H. Vozmediano, Nucl. Phys. B 424, 595 (1994); Phys. Rev. B 59, R2474 (1999).
[41] A. Giuliani, V. Mastropietro and M. Porta, Phys. Rev. B 82, 121418(R) (2010); Annals of Phys. 327, 461-511 (2012).
[42] E. G. Mishchenko, Europhys. Lett. 83, 17005 (2008).

[43] I. Herbut, V. Juričić and O. Vafek, *Phys. Rev. Lett.* **100**, 046403 (2008); V. Juričić, O. Vafek and I. Herbut, *Phys. Rev. B* **82**, 235402 (2010); I. Herbut, V. Juričić, O. Vafek and M.J. Case, arXiv:0809.0725.
[44] D. E. Sheehy and J. Schmalian, Phys. Rev. B 80, 193411 (2009).
[45] A. Giuliani and V. Mastropietro, Phys. Rev. B 85, 045420 (2012)
[46] I. Sodemann and M. M. Fogler, Phys. Rev. B 86, 115408 (2012).
[47] B. Rosenstein, M. Lewkowicz, T. Maniv, Phys. Rev. Lett. 110, 066602 (2013).
[48] I. F. Herbut and V. Mastropietro, Phys. Rev. B 87, 205445 (2013).
[49] `hhtop`, v1.0, `http://ian.jauslin.org/software/hhtop`.
[50] A. C. Curtis and P. Rabinowitz, Mathematics of Computation, 26, 117 (1972).